International Journal of Mechanical Sciences 50 (2008) 1519–1525

Contents lists available at ScienceDirect

International Journal of Mechanical Sciences

journal homepage: www.elsevier.com/locate/ijmecsci

Response of frictional receding contact problems to cyclic loading

Young Ju Ahn, J.R. Barber *

Department of Mechanical Engineering, University of Michigan, Ann Arbor, MI 48109-2125, USA

ARTICLE INFO

Article history:
Received 27 November 2007
Received in revised form
5 August 2008
Accepted 6 August 2008
Available online 13 August 2008

Keywords:
Receding contact
Coulomb friction
Shakedown
Cyclic loading

ABSTRACT

Dundurs [Properties of elastic bodies in contact. In: de Pater AD, Kalker JJ, editors. The mechanics of the contact between deformable bodies. Delft: Delft University Press; 1975. p. 54–66] has shown that if the contact area in a frictionless elastic system under load is equal to or smaller than that before loading (i.e. the contact is *receding*), the extent of the contact area is load-independent and the stress field varies linearly with load. Similar results apply to problems with Coulomb friction as long as the loading is monotonic, but otherwise non-linearities and variation in the contact area occur. In this paper, we examine this effect for the simple case of an elastic block pressed against a frictional rigid plane. During unloading there is continuous variation of both contact and slip/stick boundaries. For the important case where the loading contains a mean and a periodic component, the system approaches a steady periodic state relatively slowly and in this final state there is continuous variation of the contact area, with the minimum (i.e. the maximum amount of separation) occurring at the minimum applied load.

1. Introduction

Fig. 1(a) shows two rectangular elastic blocks pressed together by a normal force. If the block is sufficiently long compared with its height, separation occurs near the two ends of the nominal contact area as shown in Fig. 1(b). This result was first predicted by Filon [1], based on the fact that a single rectangular block loaded by two equal and opposite forces would experience a tensile stress near the edges. Later Coker and Filon [2] showed by photoelastic studies that the contact semi-width is approximately 1.35 times the block thickness. A finite element solution of this problem has since been given by Kauzlarich and Greenwood [4]. A related problem for an elastic layer pressed against an elastic substrate was treated by Keer et al. [5].

Problems of this class, in which the contact area Γ_C under load is included within the contact area Γ_0 in the unloaded state ($\Gamma_C \in \Gamma_0$) were described as *receding contact problems* by Dundurs and Stippes [6]. They possess the interesting characteristic that the stress and displacement fields are linearly proportional to the applied loads, despite the fact that the problem definition includes the unilateral contact inequalities. In particular, the extent of the contact area Γ_C is independent of the load—it immediately jumps to the loaded value as soon as an infinitesimal load is applied and remains at that value on subsequent increased loading.

The proof of this result is very simple [7]. Suppose the stresses $\boldsymbol{\sigma}$, displacements $\boldsymbol{u}$ and the contact area Γ_C are known for any particular load P. In particular, this implies that the normal tractions τ_n are compressive throughout Γ_C and that the gap is positive throughout $\Gamma_0 - \Gamma_C$. Now postulate that the corresponding solution for a load λP is $\lambda\boldsymbol{\sigma}, \lambda\boldsymbol{u}, \Gamma_C$, where λ is a scalar multiplier. Clearly this solution satisfies all the governing equations of the problem and if the normal tractions τ_n are compressive, so also will be $\lambda\tau_n$ as long as $\lambda > 0$. Similarly, if the gap derived from $\boldsymbol{u}$ is positive, that derived from $\lambda\boldsymbol{u}$ will also be positive. Thus, the inequalities are also satisfied and the initial postulate is confirmed.

1.1. Coulomb friction

The same argument can be applied to problems involving Coulomb friction as long as the loading is monotonic in time [8]. In this case Γ_C must be subdivided into a slip region Γ_S and a stick region $\Gamma_C - \Gamma_S$. In Γ_S, we have the additional condition

$$\boldsymbol{\tau}_s = -\frac{f\dot{\boldsymbol{u}}\tau_n}{|\dot{\boldsymbol{u}}|}, \tag{1}$$

where f is the coefficient of friction and the dot denotes differentiation with respect to time t. This condition states that the tangential traction $\boldsymbol{\tau}_s$ (which is a vector in the contact plane in a three-dimensional problem) must oppose the instantaneous sliding velocity $\dot{\boldsymbol{u}}$. In the stick region $\Gamma_C - \Gamma_S$, we have

$$\dot{\boldsymbol{u}} = 0; \quad |\boldsymbol{\tau}_s| < f\tau_n. \tag{2}$$

* Corresponding author. Tel.: +1 734 936 0406; fax: +1 734 615 6647.
E-mail address: jbarber@umich.edu (J.R. Barber).

0020-7403/$ - see front matter © 2008 Elsevier Ltd. All rights reserved.
doi:10.1016/j.ijmecsci.2008.08.003

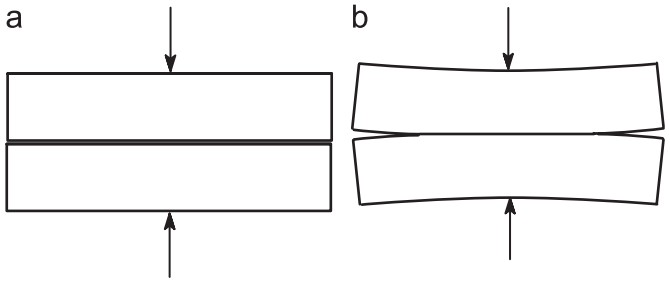

Fig. 1. Two rectangular elastic blocks compressed by a normal force: (a) unloaded and (b) loaded configuration.

Suppose that the load is given by $\lambda(t)P$ and we postulate that the corresponding displacements and tractions can be written in the form $\lambda(t)\boldsymbol{u}$, $\lambda(t)\boldsymbol{\tau}$, respectively, where $\boldsymbol{u}$, $\boldsymbol{\tau}$ and Γ_C, Γ_S are independent of time. If these expressions are substituted into the governing equations and inequalities, the factor $\lambda(t)$ will cancel in all except Eq. (1), which reduces to

$$\boldsymbol{\tau}_s = -\frac{f\dot{\lambda}\boldsymbol{u}\tau_n}{|\dot{\lambda}||\boldsymbol{u}|}. \tag{3}$$

It follows that the initial postulate is confirmed as long as $\dot{\lambda}$ retains the same sign and hence that the loading is monotonic in time.

1.2. Unloading

If the loading is non-monotonic, the previous results imply that the extent of the stick, slip and separation regions will generally differ from those during loading. This behaviour is illustrated by the solution due to Spence [9] and Turner [10] for the loading and subsequent unloading of a rigid flat cylindrical punch indenting an elastic half space. No separation occurs in this problem, but during loading ($\dot{P}>0$), radially inward slip occurs in an annular slip zone surrounding a central stick zone whose radius is independent of the load P, depending only on Poisson's ratio for the half space [9]. When the load reaches a maximum value and starts to decrease, a more complex pattern of stick and slip zones is developed. Initially, the central stick zone shrinks with decreasing load and a surrounding annulus of stick is developed at the edge. Then an outer annulus of reversed slip develops, eventually spreading inwards across the entire contact region [10].

An important case of frictional loading and unloading is that in which a contact is subjected to a combination of mean and oscillating load. Under these conditions, the long term behaviour might involve *shakedown* [11] (no slip after an initial transient), *cyclic slip* (where there is completely reversed microslip in some regions) or *ratchetting*, where the stress cycle repeats itself, but where a rigid-body displacement accumulates during each loading cycle [12]. Cyclic slip is of concern in practical applications because the microslip, which typically occurs in a region adjacent to the edge of the contact area, can lead to failure due to fretting fatigue [13].

In the present paper, we shall use a numerical method to examine the response of a receding contact problem to a combination of mean and oscillating loads. We shall verify that the slip and separation zones remain unchanged throughout the first loading phase, but thereafter all the zone boundaries vary during both loading and unloading periods. Eventually a steady periodic state is achieved.

2. Problem description

We consider the two-dimensional problem illustrated in Fig. 2, in which a rectangular elastic body of height h and width $4h$ is pressed against a rigid plane surface by a uniform time-varying pressure $p_0(t)$ exerted over a central strip of width $2h$ on the upper surface. This example shares many of the features of the receding contact problems discussed by previous authors. However, in contrast to Filon's problem of Fig. 1, the contact interface is not a plane of symmetry, implying that we should expect coupling between normal and tangential effects. Coulomb friction boundary conditions are assumed at the interface between the block and the plane, with friction coefficient f. We assume that the loading is sufficiently slow for the quasi-static analysis to be appropriate, in which case time t appears only as an evolutionary parameter describing the sequence of the loading.

The deformation of the block is analysed by the finite element method and in particular the contact surface is defined by a set of N nodes, $i=1,N$. The normal and tangential nodal reaction forces acting on the block will be denoted by P_i, Q_i, respectively, with the convention that P_i is positive when compressive and Q_i is positive in the positive x-direction, as shown in Fig. 2. The corresponding vertical and horizontal nodal displacements are denoted by w_i, v_i, respectively.

At any time t, node i must be in one of the four states:

(1) *Stick*: The node is in contact and there is no relative motion, so

$$w_i = 0; \quad \dot{v}_i = 0. \tag{4}$$

For this state to hold, the normal reaction must be compressive and the tangential reaction must satisfy the Coulomb friction inequality, giving

$$P_i > 0; \quad -fP_i \leqslant Q_i \leqslant fP_i. \tag{5}$$

(2) *Separation*: The node is not in contact, so the reaction forces are both zero, giving

$$P_i = Q_i = 0. \tag{6}$$

For this to hold, the gap between the block and the plane surface must be non-negative, which requires

$$w_i \geqslant 0. \tag{7}$$

(3) *Forward slip*: The node is in contact and slipping to the right, so

$$w_i = 0; \quad \dot{v}_i > 0. \tag{8}$$

The normal contact reaction must be compressive and the Coulomb friction law implies that Q_i opposes the motion, giving

$$P_i > 0; \quad Q_i = -fP_i. \tag{9}$$

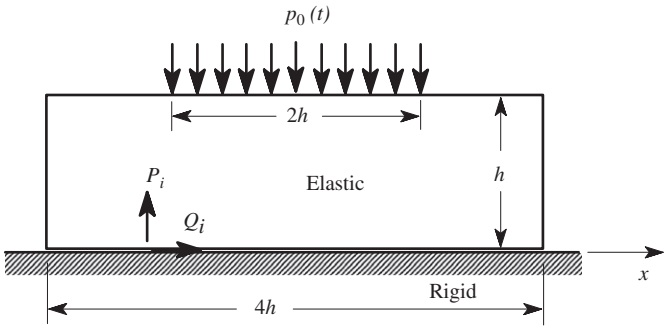

Fig. 2. A rectangular elastic block pressed against a rigid plane surface.

(4) *Backward slip*: The node is in contact and slipping to the left, so

$$w_i = 0; \quad \dot{v}_i < 0; \quad P_i > 0 \quad \text{and} \quad Q_i = fP_i. \tag{10}$$

2.1. Solution procedure

Following [11], we can write the vector of nodal reaction forces in the form

$$\boldsymbol{r} = \boldsymbol{r}^* + \boldsymbol{K}\boldsymbol{u}, \tag{11}$$

where

$$\boldsymbol{r} = \begin{Bmatrix} \boldsymbol{Q} \\ \boldsymbol{P} \end{Bmatrix}; \quad \boldsymbol{K} = \begin{bmatrix} \boldsymbol{K}_{tt} & \boldsymbol{K}_{tn} \\ \boldsymbol{K}_{nt} & \boldsymbol{K}_{nn} \end{bmatrix}; \quad \boldsymbol{u} = \begin{Bmatrix} \boldsymbol{v} \\ \boldsymbol{w} \end{Bmatrix}; \quad \boldsymbol{r}^* = \begin{Bmatrix} \boldsymbol{Q}^* \\ \boldsymbol{P}^* \end{Bmatrix} \tag{12}$$

and $P_i^*(t)$, $Q_i^*(t)$ are the time-varying nodal reaction forces that would be generated by the given external load $p_0(t)$ if all the nodes were restrained from moving. These forces can be found by a finite element solution of the problem of Fig. 2 under the boundary conditions $\boldsymbol{u} = 0$.

The stiffness matrix $\boldsymbol{K}$ can be found from the finite element discretization of Fig. 2 using a standard condensation procedure. It is symmetric and hence $\boldsymbol{K}_{nn}$, $\boldsymbol{K}_{tt}$ are also symmetric. The normal–tangential coupling matrices $\boldsymbol{K}_{nt}$, $\boldsymbol{K}_{tn}$ are generally not symmetric, but they obey the relation

$$\boldsymbol{K}_{tn} = \boldsymbol{K}_{nt}^{\mathrm{T}}. \tag{13}$$

The solution of the transient loading problem under any transient loading $p_0(t)$ can then be stated and solved in terms

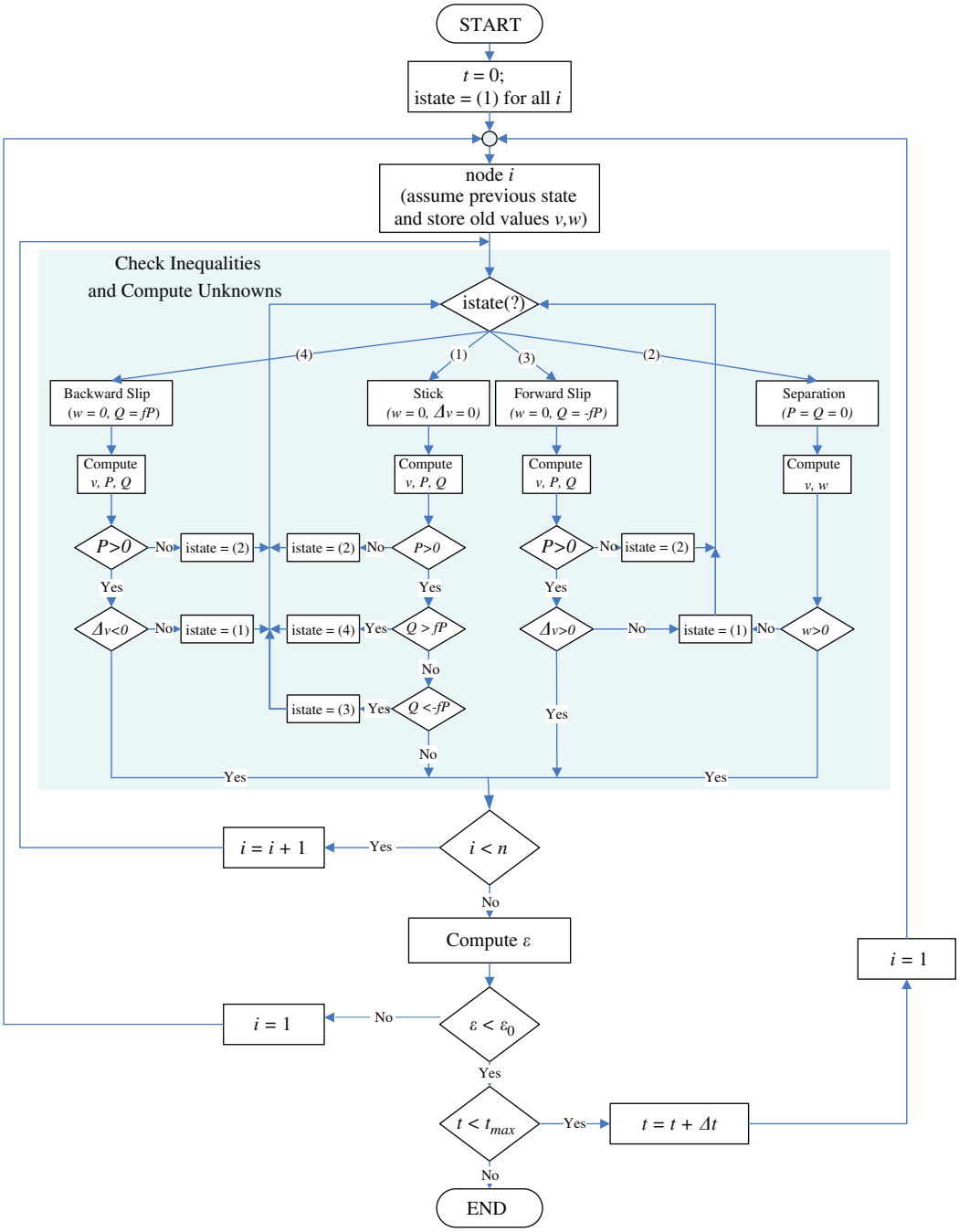

Fig. 3. Solution algorithm.

of the variables defined in Eq. (12), making use of the state Eqs. (4)–(10).

The problem is solved at a series of time increments t_j in which case the stick condition $\dot{v}_i = 0$ (4) translates to the condition

$$v_i(t_{j+1}) = v_i(t_j) \tag{14}$$

and the frictional inequalities $\dot{v}_i > 0$ (8) and $\dot{v}_i < 0$ (10) translate to

$$v_i(t_{j+1}) > v_i(t_j) \quad \text{and} \quad v_i(t_{j+1}) < v_i(t_j) \tag{15}$$

respectively. Thus, if the state of the system is completely known at time t_j, Eqs. (4)–(10) provide a set of conditions sufficient to determine the state at time t_{j+1}.

2.2. Solution algorithm

The numerical solution is obtained by a Gauss–Seidel procedure whereby the displacements at each node are updated one by one, assuming that those at other nodes remain unchanged. At each time step, the algorithm cycles through the entire set of contact nodes several times until the governing equations at all nodes are satisfied to within a set tolerance. A block diagram of the algorithm is given in Fig. 3.

For the update procedure, the state (stick, forward slip, backward slip or separation) at the node in question is assumed to be that for the previous iteration. The corresponding equations are then solved and the appropriate inequalities are checked. If the inequalities are not satisfied, the state assumption is changed and the node is solved again.

We should remark at this point that the system 'memory' is entirely contained in the instantaneously locked-in displacements in the stick regions and this memory is acquired at times when any node makes the transition from slip or separation to stick. Such a transition may actually be indicated at a time between t_j and t_{j+1} and hence the accuracy of the stored displacements depends on the time step (or more strictly the loading increment) being small enough for this to have a negligible effect on the solution. When the transition occurs from separation to stick, a better approximation is achieved by first identifying the position of the node predicted under the zero traction assumption. If there is to be a transition to contact, this will involve a negative gap. By assuming a linear trajectory from the previous position of the node, we can estimate the point of first contact and use this for the tangential nodal displacement at the newly stuck node.

The iteration at each time step is terminated when the changes $\Delta v_i, \Delta w_i$ in the displacements v_i, w_i at all slipping and separated nodes during the last iteration are less than a given proportion of the corresponding displacement. In other words, when $\mathscr{E} < \mathscr{E}_0$, where

$$\mathscr{E} = \max_{v_i, w_i}\left(\frac{\Delta v_i}{v_i}, \frac{\Delta w_i}{w_i}\right). \tag{16}$$

Convergence of the finite element description was tested by refining the mesh until the incremental changes in contact tractions and slip and stick zones were not detectable in appropriate plots of the results. It was found that a mesh with 25,600 elements and 321 contact nodes gave acceptable accuracy by this criterion.

3. Results

Results were obtained for the case where the external load $p_0(t)$ initially increases with time to a maximum value $p_0^{\max}$, after which it is monotonically reduced to zero. The coefficient of friction was taken to be $f = 0.35$ and Poisson's ratio $\nu = 0.3$.

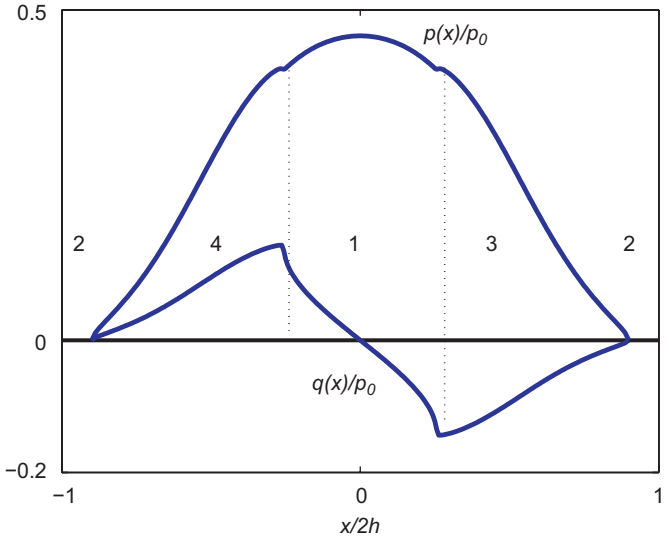

Fig. 4. Normalized contact traction distributions during the initial loading. Numbers refer to the four states defined in Section 2.

During the initial loading phase, separation occurs at the edges of the block and the contact area comprises a central stick zone flanked by regions of forward and backward slip. The extent of these zones remains constant throughout the loading phase and the normal and shear tractions retain the same form and increase proportionally with the load, as predicted in Section 1.1. Fig. 4 shows the distributions of normal traction $p(x)$ and shear traction $q(x)$, normalized by the instantaneous value of $p_0(t)$.

3.1. Unloading

When the load starts to decrease from its maximum value, the immediate effect is for a stick zone to be developed at the edges of the contact, but two interior slip regions remain. Fig. 5 shows the evolution of the stick, slip and separation regions during the unloading process. As in Turner's indentation problem [10], regions of slip are developed at the edge of the contact area opposite in sign to the slip that occurred during loading, whilst the interior slip regions extend inwards at the expense of the central stick region. Notice that the five central zones (stick/forward slip/stick/backward slip/stick) all tend to zero near the end of the unloading process. This is necessary since if we track the state at a point that is stuck during loading and that experiences forward slip during unloading, it must eventually also experience a period of backward slip, since at complete unloading the total slip displacement must revert to zero. A new feature in this problem is that the total contact area itself decreases monotonically relative to the fully loaded state (the two separation regions extend). This continues until the instant of complete unloading when the gap at all points in the separation zone goes to zero. Notice also that the inner boundaries of the two outer stick zones (1) in Fig. 5 move inwards during unloading, implying that the stick zone is 'advancing' and hence that the instantaneous state depends on the complete history of unloading and not merely on the instantaneous load [14]. Fig. 6 shows the normalized traction distributions at $p_0(t) = p_0^{\max}/3$ during the unloading process.

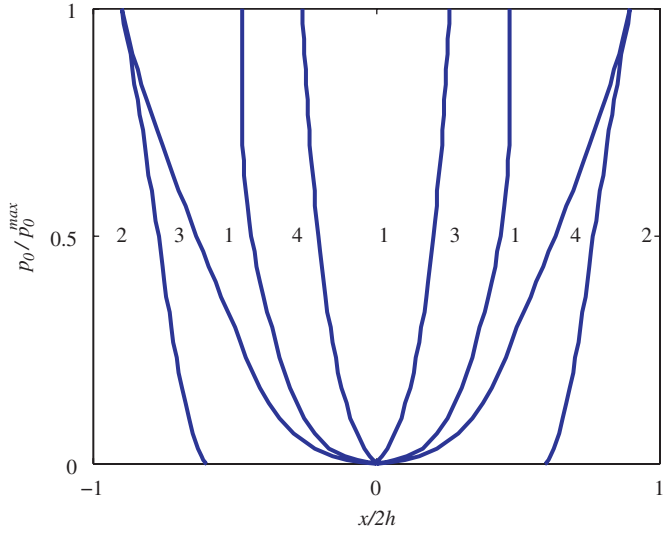

Fig. 5. Evolution of stick (1), separation (2), forward slip (3) and backward slip (4) regions during unloading.

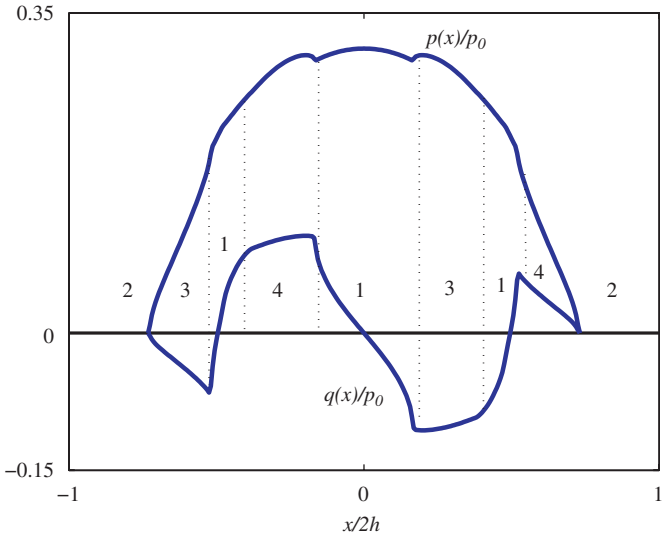

Fig. 6. Normalized contact traction distributions during unloading.

3.2. Oscillatory loading

We next consider the case where the load is first increased to the maximum value p_0^{max}, after which it oscillates in the range $p_0^{max} > p_0(t) > p_0^{max}/3$. Other values for the minimum load were also examined and found to give qualitatively similar results. The first loading and unloading cycle is of course similar to that presented in Section 3.1 and the traction distribution when the load is first reduced to $p_0^{max}/3$ is given by Fig. 6 as before. However, during the reloading phase, the tractions and the extent of the stick, slip and separation zones follow a new scenario and the cycle continues to evolve over subsequent cycles. This contrasts with previous studies of frictional systems subject to oscillatory loading, where the steady cyclic state is generally reached after only a few cycles [3].

Figs. 7(a, b) show the evolution of the slip, stick and separation regions during the unloading and reloading phases, respectively, after nine cycles of loading. The extent of the separation zone varies during the cycle and points near the edge of the contact area experience cyclic slip. Notice in particular that during unloading, the three stick regions (1) are separated by small regions of slip, indicated by arrows in Fig. 7(a). These regions remain stuck during reloading and this is a clear indication that the steady state has not yet been reached, since the magnitude of the accumulated slip displacement v_i in these regions continues to

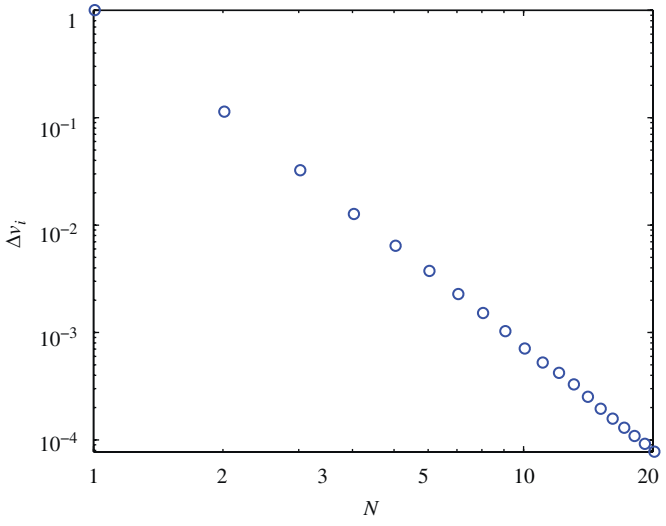

Fig. 8. Incremental slip Δv_i per cycle at a representative node as a function of cycle number N.

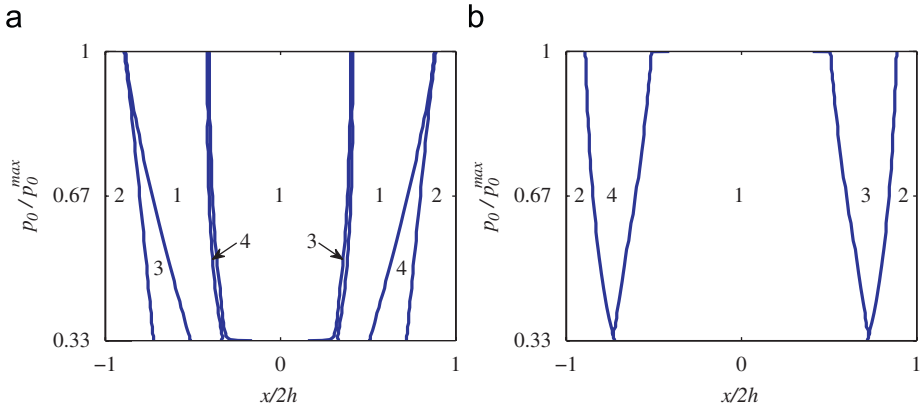

Fig. 7. Evolution of the stick, slip and separation regions during the ninth cycle of (a) unloading and (b) reloading.

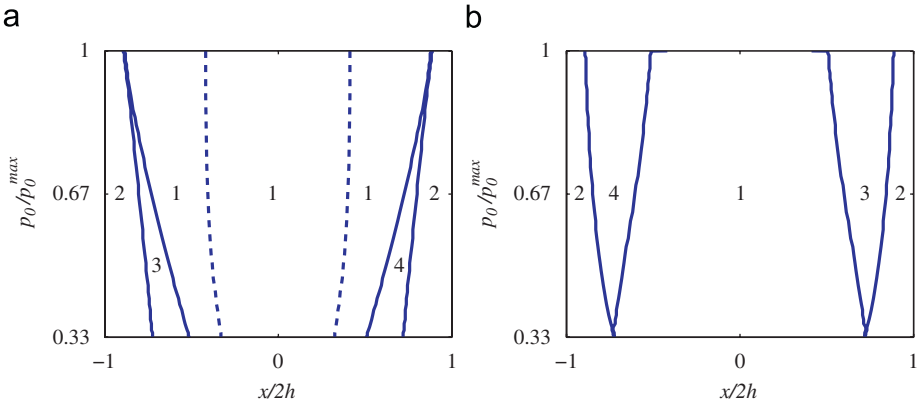

Fig. 9. Evolution of the stick, slip and separation regions during (a) unloading and (b) reloading in the steady cyclic state. The dashed line in (a) indicates points which reach the limiting friction condition but which do not actually slip.

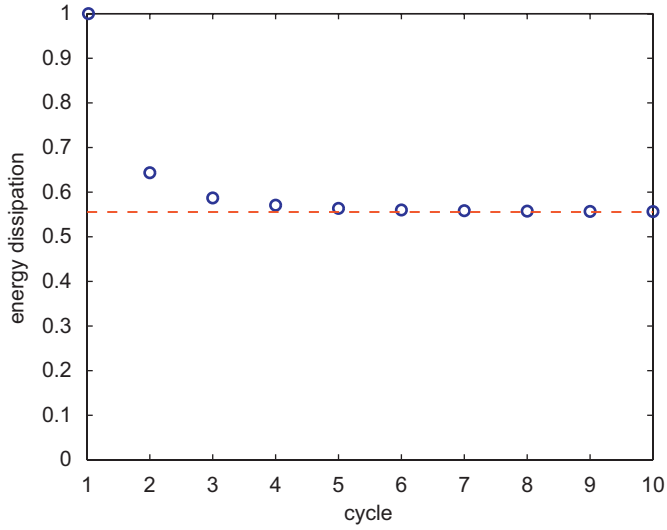

Fig. 10. Evolution of the energy dissipated in friction per loading cycle as a proportion of that during the first cycle.

increase monotonically with each cycle. However, the increment Δv_i in slip displacement per cycle decreases with the number of cycles elapsed N. Results for a representative node are shown in Fig. 8 and show that $\Delta v_i \sim N^{-3.1}$. Eventually Δv_i falls within the tolerance of the numerical algorithm, but if this trend were assumed to continue indefinitely (given arbitrarily high levels of numerical precision), the increments Δv_i would have a finite sum representing a steady state that is approached monotonically and asymptotically.

The evolution of slip, stick and separation regions during unloading and reloading in the final steady state is shown in Figs. 9(a, b). The dashed line in Fig. 9(b) denotes a range of points that achieve the limiting friction condition $|Q| = fP$ at some point during the cycle, but at which no slip actually occurs. This phenomenon was also noted by Dini and Hills [15].

The extent of the cyclic slip zones in the steady state is smaller than in the earlier phases of loading, showing that some degree of shakedown has occurred. This effect is quantified in Fig. 10 where we present the evolution of the normalized energy dissipation per cycle, which is a parameter that is expected to correlate with fretting damage. The energy dissipation per cycle decreases monotonically with each cycle and it seems likely that this would be true for all frictional systems, though the present authors are unaware of a proof of this result. The steady-state energy dissipation is approximately 56% of that during the first loading cycle.

4. Conclusions

Dundurs' results for receding contact problems can be extended to problems involving Coulomb friction, but only as long as the loading is monotonic. During unloading, changes occur in the extent of both separation and slip zones. We have illustrated this behaviour for the case of an elastic block pressed against a frictional rigid plane. In particular, we find that if the load is periodic in time, the system approaches a steady periodic state relatively slowly and in this final state there is continuous variation of the contact area, with the minimum (i.e. the maximum amount of separation) occurring at the minimum applied load. The system exhibits some degree of shakedown in the sense that the energy dissipation decreases monotonically towards a steady-state limit with each successive cycle.

Acknowledgment

Young Ju Ahn wishes to thank the Electric Power National Scholarship Program of the Korean Ministry of Commerce, Industry and Energy (MOCIE) for financial support.

References

[1] Filon LNG. On an approximate solution for the bending of a beam of rectangular cross-section under any system of load. Philosophical Transactions of the Royal Society of London 1903;206A:63–155.
[2] Coker EG, Filon LNG. A treatise on photoelasticity. Cambridge: Cambridge University Press; 1957.
[3] Karuppanan S, Hills DA. Frictional complete contacts between elastically similar bodies subject to normal and shear load. International Journal of Solids and Structures 2008;45:4662–75.
[4] Kauzlarich JJ, Greenwood JA. Contact between a centrally loaded plate and a rigid or elastic base, with application to pivoted pad bearings. Journal of Mechanical Engineering Science 2001;215:623–8.
[5] Keer LM, Dundurs J, Tsai KC. Problems involving a receding contact between a layer and a half-space. ASME Journal of Applied Mechanics 1972;39:1115–20.
[6] Dundurs J, Stippes M. Role of elastic constants in certain contact problems. ASME Journal of Applied Mechanics 1970;37:965–70.
[7] Dundurs J. Properties of elastic bodies in contact. In: de Pater AD, Kalker JJ, editors. The mechanics of the contact between deformable bodies. Delft: Delft University Press; 1975. p. 54–66.
[8] Ciavarella M, Baldini A, Barber JR, Strozzi A. Reduced dependence on loading parameters in almost conforming contacts. International Journal of Mechanical Sciences 2006;48:917–25.
[9] Spence DA. An eigenvalue problem for elastic contact with finite friction. Proceedings of the Cambridge Philosophical Society 1973;73:249–68.

[10] Turner JR. Frictional unloading problem on a linear elastic half-space. Journal of the Institute of Mathematics and its Applications 1979;24: 439–69.
[11] Klarbring A, Ciavarella M, Barber JR. Shakedown in elastic contact problems with Coulomb friction. International Journal of Solids and Structures 2007; 44:8355–65.
[12] Mugadu A, Sackfield A, Hills DA. Analysis of a rocking and walking punch—part I: initial transient and steady state. ASME Journal of Applied Mechanics 2004;71:225–33.
[13] Nowell D, Dini D, Hills DA. Recent developments in the understanding of fretting fatigue. Engineering Fracture Mechanics 2006;73:207–22.
[14] Hills DA, Kelly PA, Dai DN, Korsunsky AM. Solution of crack problems—the distributed dislocation technique. Dordrecht, The Netherlands: Kluwer Academic Publishers; 1996.
[15] Dini D, Hills DA. Unsymmetrical shear loading and its influence on the frictional shakedown of incomplete contacts. Proceedings of the Institution of Mechanical Engineers Part C—Journal of Mechanical Engineering Science 2004;218:469–75.